ISSN 0018-151X, High Temperature, 2022, Vol. 60, Suppl. 2, pp. S187–S193. © Pleiades Publishing, Ltd., 2022.
Russian Text © The Author(s), 2021, published in Teplofizika Vysokikh Temperatur, 2021, Vol. 59, No. 5, pp. 693–700.

THERMOPHYSICAL PROPERTIES OF MATERIALS

Viscoelastic and Quasi-Solid Properties of Ni-Containing Binary Metal Melts

R. M. Khusnutdinoff[a, b, *], R. R. Khairullina[a], A. L. Bel'tyukov[a, b], V. I. Lad'yanov[b], and A. V. Mokshin[a, b, **]

[a] *Kazan (Volga region) Federal University, Kazan, Russia*

[b] *Udmurt Federal Research Center of the Ural Branch of the Russian Academy of Sciences, Izhevsk, Russia*

**e-mail: khrm@mail.ru*

***e-mail: anatolii.mokshin@mail.ru*

Received September 3, 2020; revised September 3, 2020; accepted May 19, 2021

Abstract—This paper investigates the viscoelastic and quasi-solid state properties of nickel-containing binary metal melts in a wide temperature range, including the region of the equilibrium liquid phase and supercooled melt. The results of experimental measurements on viscometry and the molecular dynamics simulation results are compared in order to refine the data on viscosity and identify the features of the quasi-solid state behavior in various nickel-containing metal melts. The simulation results for the concentration and temperature dependences of viscosity are in close agreement with the experimental data. It is established that a significant increase in viscosity is observed at nickel concentrations of $x_{Ni} = 60–80\%$ and 30–50% for $Al_{(100-x)}Ni_x$ and $Fe_{(100-x)}Ni_x$ melts, respectively. In addition, in the region of low concentrations ($x_{Ni} \sim 5\%$), pronounced features are observed both in shear and kinematic viscosity for iron-nickel melts. The elastic properties are analyzed in detail based on the numerical calculations of the bulk compression and shear moduli, Poisson's ratio, and Young's modulus. It is shown that with a change in the concentration of nickel in $Fe_{(100-x)}Ni_x$ and $Al_{(100-x)}Ni_x$ systems, the elastic moduli change by factors of two and three, respectively. The calculated values of the concentration dependences of the longitudinal and transverse sound velocities show a correlation with viscosity. It is found that at concentrations of $x_{Ni} \le 60\%$, $Fe_{(100-x)}Ni_x$ melts are characterized by more pronounced solid-like properties compared to $Al_{(100-x)}Ni_x$ melts.

DOI: 10.1134/S0018151X21050096

INTRODUCTION

Nickel-containing binary metal systems, such as aluminum-nickel and iron-nickel alloys, are widely used in mechanical engineering and the aircraft industry due to their unique physical and mechanical properties [1]. The Al–Ni alloy is the base system for technologically important superalloys, which are widely used as high-temperature materials (for example, for turbine blades in aircraft engines). Amorphous and nanostructured alloys based on Al–Ni are characterized by mechanical properties correlated with microhardness and wear resistance [2]. Nickel-based alloys also have excellent anticorrosion properties. Products made from such alloys are mainly in demand in the oil and gas, as well as energy, industries.

Binary iron-nickel alloys consisting of two ferromagnetic elements—iron (with a magnetic moment $\mu = 2.2\mu_B$ and Curie temperature $T_C = 1044$ K, where μ_B is the Bohr magneton) and nickel ($\mu = 0.64\mu_B$ and $T_C = 624$ K)—demonstrate unique strength, physicomechanical, and magnetic properties over the entire concentration range. For example, amorphous metal alloys based on iron and nickel are good soft magnetic materials [3]. The main structural component of such alloys is the intermetallic compound $FeNi_3$ [4]. The effect of introducing nickel into the main structure of the alloy is that the thermal strength increases in such an alloy. These alloys are used in parts that operate for a long time in aggressive environments. They have increased mechanical strength and resistance at high temperatures and external mechanical loads.

To develop materials with the desired characteristics, it is very important to know the structural features and physicochemical properties of molten systems before solidification. An important physical characteristic of any liquid is its viscosity, which can be determined directly in experiments and quite correctly calculated using molecular dynamics simulations [5]. Viscosity is one of the most important characteristics that determines the relaxation features, thermophysical, and transport properties of a substance, it is highly sensitive to structural transformations and phase transitions, and also plays an important role in the kinetics of chemical reactions [6, 7]. At the same time, the nature of the temperature dependence of viscosity determines the so-called amorphous ability of the system [8]. Indirect experimental techniques, such as inelastic scattering of neutrons, X-rays, Brillouin scattering of light, are characterized by significant inaccu-

racies in determining the transport coefficients (diffusion, viscosity). At the same time, the determination of viscosity using viscometry methods—capillary viscometry, torsional vibration method, ultrasonic method, etc.—is associated with significant difficulties, primarily due to the low sensitivity and imperfection of these methods [9]. An alternative way to determine viscosity is provided by classical and quantum mechanical simulation methods. The results obtained using the methods of classical modeling depend significantly on the correctness of the chosen interatomic interaction potential. The results of quantum mechanical simulation depend on the approximations used in the exchange-correlation potential. Thus, the refinement of absolute values and the development of universal models of viscosity are one of the important tasks of modern thermal physics and the physics of condensed matter [5].

In this study, experimental data and the results of molecular dynamics studies are compared in order to refine the data on temperature and concentration[1] viscosity dependences of nickel-containing binary metal systems, including the area of the equilibrium liquid and supercooled melt. Another goal of this study is a detailed analysis of the elastic and quasi-solid properties of high-temperature melts of $Al_{(100-x)}Ni_x$ and $Fe_{(100-x)}Ni_x$.

DETAILS OF SIMULATION

The molecular dynamics of nickel-containing metal $Al_{(100-x)}Ni_x$ and $Fe_{(100-x)}Ni_x$ melts are simulated in an NpT ensemble under the pressure p = 1.0 bar for the temperature range T = [1200; 2000] K, which covers the areas of the equilibrium liquid phase and the supercooled state. The studied systems consisted of N = 32000 atoms, located in a cubic cell with periodic boundary conditions. Interactions between atoms were carried out using embedded atom potentials (EAM potentials) [10] and [11], respectively. Melts with given temperatures were obtained by rapid cooling from a high-temperature equilibrium state at T= 3000 K. The equations of motion of the atoms were integrated using the velocity Verlet algorithm in with a time step of 1.0 fs [12]. To bring the systems into a state of thermodynamic equilibrium, the program performed 1.5×10^7 time steps and 2×10^8 steps for calculating the time correlation functions, elastic properties, and quasi-solid state characteristics.

DESCRIPTION OF THE EXPERIMENT

Al–Ni alloys are obtained by alloying high-purity aluminum and $Al_{99}Ni_1$ or $Al_{85}Ni_{15}$ alloys in a viscometer furnace in a high-purity helium atmosphere at a temperature of T = 1373 K and isothermal holding for at least 1 h. When smelting alloys with the nickel content ranging from 1 to 9 at %, an $Al_{85}Ni_{15}$ ligature was used; and when smelting alloys with a nickel content of less than 1 at %, an $Al_{99}Ni_1$ ligature was used. The ligatures were obtained by fusing metals in a resistance furnace at a residual pressure of 10^{-2} Pa and temperature T = 1943 K for 30 min. The initial components were highly pure aluminum (99.999 wt % Al) and electrolytic nickel (99.5 wt % Ni). The nickel content in the alloys was determined by atomic emission spectroscopy on a SPECTROFlameModula D spectrometer. The kinematic viscosity of the melts was measured on an automated installation by the method of torsional vibrations [13, 14]. The measurements were carried out in a protective atmosphere of purified helium. Cylindrical Al_2O_3 cups with an inner diameter of 17 mm and a height of 40 mm were used as the crucibles. A lid was placed in the crucible over the sample. The lids were made from cups made of Al_2O_3 12 mm high, with the outer diameter of 0.4 to 0.6 mm less than the inner diameter of the crucible. The design of a crucible with a lid is given in [15]. The lid can move along the vertical axis of the crucible and thereby compensate the changes in the sample volume. When performing torsional vibrations, the cover moves together with the crucible, creating an additional end surface of friction with the melt. The crucibles and lids were preliminarily annealed in a vacuum furnace at a residual pressure of 10^{-2} Pa, temperature T = 1923 K, and isothermal exposure for 1 h. The use of a crucible with a lid for measuring viscosity makes it possible to exclude the influence of film effects and wetting phenomena on the measurements [16]. Before taking the measurements, all the samples were remelted at a temperature of 1473 K in a viscometer furnace with subsequent cooling to room temperature. The temperature dependences of the viscosity were obtained in heating modes from the liquidus temperature of the alloy up to 1473 K and subsequent cooling until the melt began to crystallize. Isothermal holding for 15 min was carried out at each temperature before the measurements were taken. The values of kinematic viscosity and the errors of its determination were calculated according to the methods described in [17, 18]. The total relative error in determining the viscosity does not exceed 4% with the error of a single experiment not exceeding 2%.

SIMULATION RESULTS AND COMPARISON WITH EXPERIMENT

The shear viscosity was calculated from the molecular dynamics simulation data using the Green–Kubo relations

$$\eta = \frac{V}{k_B T}\int_0^\infty \langle \sigma_{\alpha\beta}(t)\sigma_{\alpha\beta}(0)\rangle\, dt,$$

where angular brackets denote averaging over time and the ensemble of particles, k_B is the Boltzmann constant, V is the volume of the system, and $\sigma_{\alpha\beta}$ are the off-diagonal components of the stress tensor. The kinematic viscosity ν was calculated as η/ρ, where ρ is

[1] Hereafter, all concentrations are given in atomic percent of nickel.

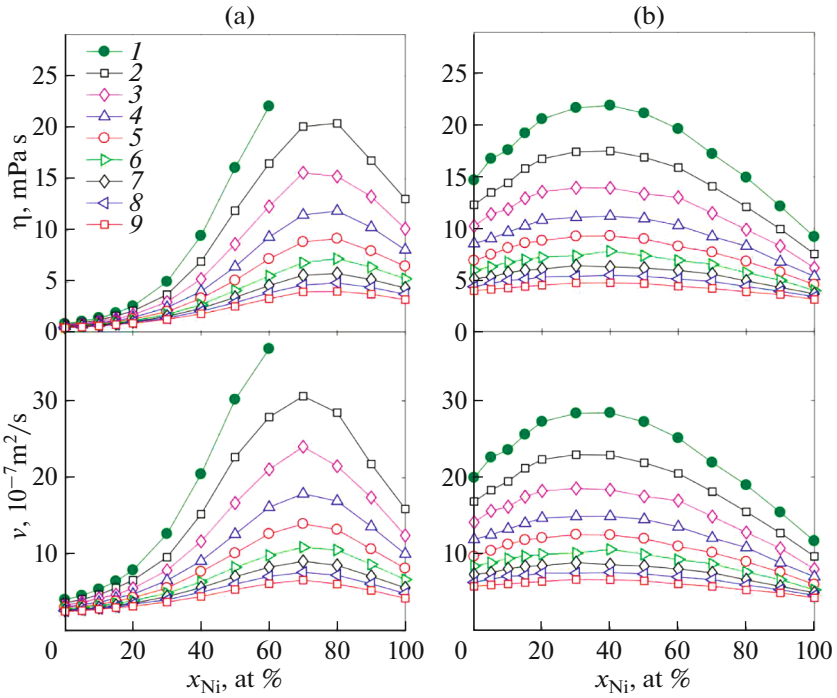

Fig. 1. Shear and kinematic viscosity of $Al_{(100-x)}Ni_x$ (a) and $Fe_{(100-x)}Ni_x$ (b) melts as a function of composition at different temperatures: (*1*) T = 1200 K, (*2*) 1300, (*3*) 1400, (*4*) 1500, (*5*) 1600, (*6*) 1700, (*7*) 1800, (*8*) 1900, (*9*) 2000.

the density of the system. Figure 1 shows the results of molecular dynamics simulations for the concentration dependences of the shear and kinematic viscosity of $Al_{(100-x)}Ni_x$ and $Fe_{(100-x)}Ni_x$ melts at various temperatures. The isotherms show viscosity the maximums at concentrations of $x_{Ni} \in [60; 80]$% for the aluminum-nickel system and at $x_{Ni} \in [30; 50]$% for the iron-nickel melts, which may be due to the presence of a number of intermetallic phases in the solid phase. Thus, in the works [19–21], for some compositions of aluminum-nickel systems, questions were discussed where an increase in viscosity is related to the possible presence of a short-range chemical order in the liquid, leading to the formation of clusters [22]. A significant increase in viscosity at low temperatures in these systems is obviously due to the slowing down of particle dynamics in the region of the supercooled melt phase. In addition, in the region of low concentrations ($x_{Ni} \sim$ 5%), features are observed both in the shear and kinematic viscosity for $Fe_{(100-x)}Ni_x$ melts, while such viscosity features for $Al_{(100-x)}Ni_x$ systems are not observed.

Figure 2a presents the results of modeling the concentration dependences of the shear viscosity coefficient for aluminum-nickel and iron-nickel (Fig. 2b) melts in comparison with the experimental data. The values of the experimental shear viscosity η were obtained as $\eta = \nu\rho$, where ν is the kinematic viscosity determined directly in the viscometry experiment. The experimental values of density ρ for $Al_{(100-x)}Ni_x$ and $Fe_{(100-x)}Ni_x$ systems are taken from [28, 29] and [30], respectively. There is close agreement between the simulation results and the results of the author's experiment on viscometry for aluminum-nickel melts at all the considered temperatures and for the entire range of the studied concentrations. The experimental data from [23] also show satisfactory agreement with the results of the author's study, while the data from [24] demonstrate worse agreement. For iron-nickel melts (Fig. 2b), the data of different experimental groups differ significantly from each other. The data differ by a factor of at least 1.5. As a consequence, the general trend in the behavior of $\eta(x)$ for $Fe_{(100-x)}Ni_x$ melts cannot be determined.

The elastic properties of amorphous metal alloys were investigated by determining the values of the elastic moduli: the modulus of compression and shear modulus. In the case of an *NpT* ensemble, the bulk compression modulus is related to the root-mean-square fluctuations σ_V^2 of volume V of the simulation cells by the expression

$$B = \frac{k_B T V}{\sigma_V^2}.$$

The shear modulus was calculated by the formula

$$G = \frac{V}{k_B T}\left|\sigma_{xy}(0)\right|^2,$$

where the angular brackets denote averaging over time samples. Figure 3a shows the results of molecular dynamics simulation for the concentration dependences of the bulk compression modulus and the shear

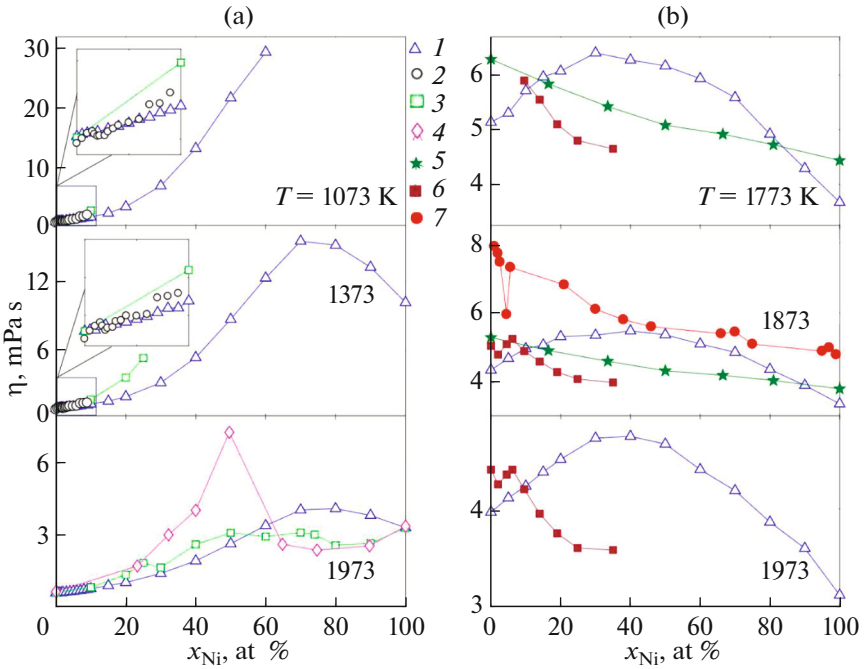

Fig. 2. Concentration dependences of shear and kinematic viscosity of aluminum-nickel (a) and iron-nickel (b) melts at different temperatures: (*1*) atomic dynamic simulations results; (*2*) results of the viscometry experiment; experimental data: (*3*) [23], (*4*) [24], (*5*) [25], (*6*) [26], (*7*) [27].

modulus of $Al_{(100-x)}Ni_x$ and $Fe_{(100-x)}Ni_x$ melts (Fig. 3b) at different temperatures.

In addition, the equilibrium modulus of elasticity (Young's modulus) and the coefficient of the transverse strain (Poisson's ratio) are calculated. Young's modulus E and Poisson's ratio σ are related to the elastic moduli by the following relations [31]:

$$E = \frac{9BG}{3B+G}, \quad \sigma = \frac{3B-2G}{6B+2G}.$$

Figure 4 shows the molecular dynamics simulation results for the concentration dependences of Poisson's ratio and Young's modulus for $Al_{(100-x)}Ni_x$ (Fig. 4a) and $Fe_{(100-x)}Ni_x$ (Fig. 4b) melts at different temperatures. The concentration regions at which the systems are characterized by more pronounced strength properties are clearly observed. Thus, for the aluminum-nickel and iron-nickel melts, these regions correspond to the concentrations of nickel atoms x_{Ni} = 60–90% and 40–80%, where the moduli reach 169 and 198 GPa, respectively.

The elastic characteristics (modules B and G) and the propagation velocities of the longitudinal and transverse ultrasonic waves for an isotropic medium are related by the expressions

$$\vartheta_L = \sqrt{\frac{B+\frac{4}{3}G}{\rho}}, \quad \vartheta_T = \sqrt{\frac{G}{\rho}}.$$

Figure 5 presents the molecular dynamics simulation results for the concentration dependences of the longitudinal and transverse sound velocities for aluminum-nickel and iron-nickel melts at different temperatures. The calculated values of the concentration dependences of the rates demonstrate a correlation with the viscosity values.

Using the simulation results for the shear viscosity and shear modulus, the relaxation time of the viscosity process τ is calculated as η/G_∞. The quasi-solid-state features of nickel-containing binary metal systems were analyzed within the framework of the Maxwell–Frenkel theory [32–34], where the gap width in the dispersion law of the transverse collective modes is defined as

$$k_{gap} = \frac{1}{2\vartheta_T\tau} = \frac{G_\infty}{2\vartheta_T\eta}.$$

Figure 6 presents the molecular dynamics simulation results for the concentration dependences of the relaxation time of the viscous process and the gap width in the law of dispersion of transverse collective modes for aluminum-nickel and iron-nickel melts at different temperatures. The relaxation time of the viscous process has a significant maximum at nickel concentrations of x_{Ni} = 60–80% for $Al_{(100-x)}Ni_x$ melts, while for the $Fe_{(100-x)}Ni_x$ system, such a feature in x_{Ni} = 30–50% is weakly expressed. We note that the anomalous behavior of the relaxation time τ and viscosity is observed at the values of $x_{Ni} \sim 5\%$. The width of the gap in the law of dispersion of transverse collective modes can be used to judge the quasi-solid-state properties of the melts. Thus, at concentrations of $x_{Ni} \le 60\%$, $Fe_{(100-x)}Ni_x$ melts are characterized by

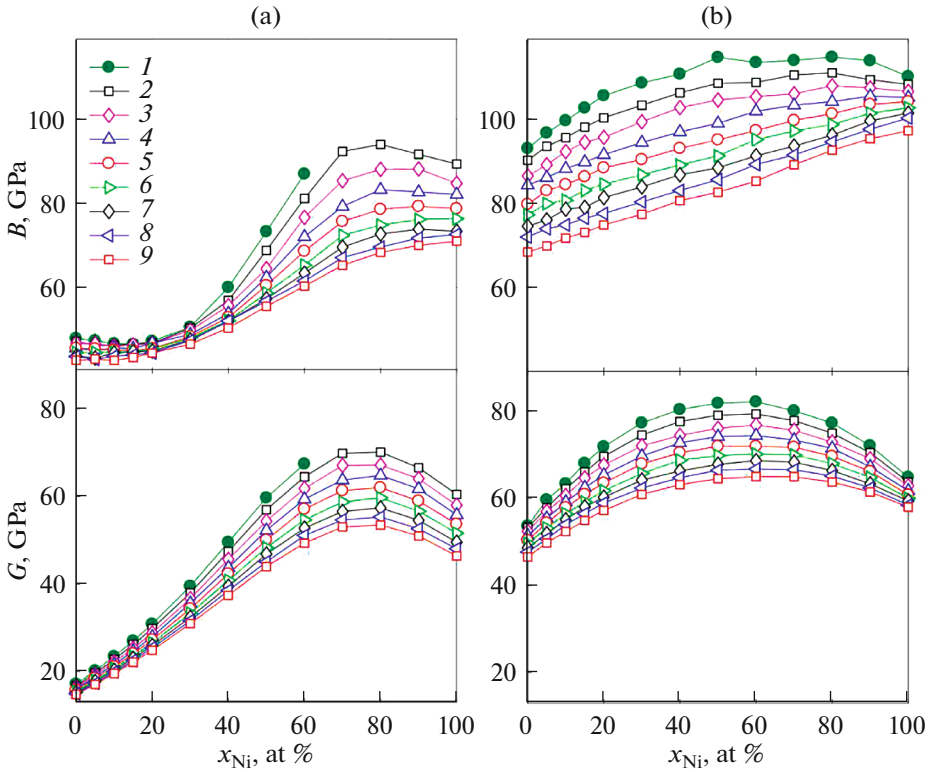

Fig. 3. Concentration dependences of the bulk compression modulus and shear modulus of $Al_{(100-x)}Ni_x$ (a) and $Fe_{(100-x)}Ni_x$ (b) melts at different temperatures: (*1*–*9*) see Fig. 1.

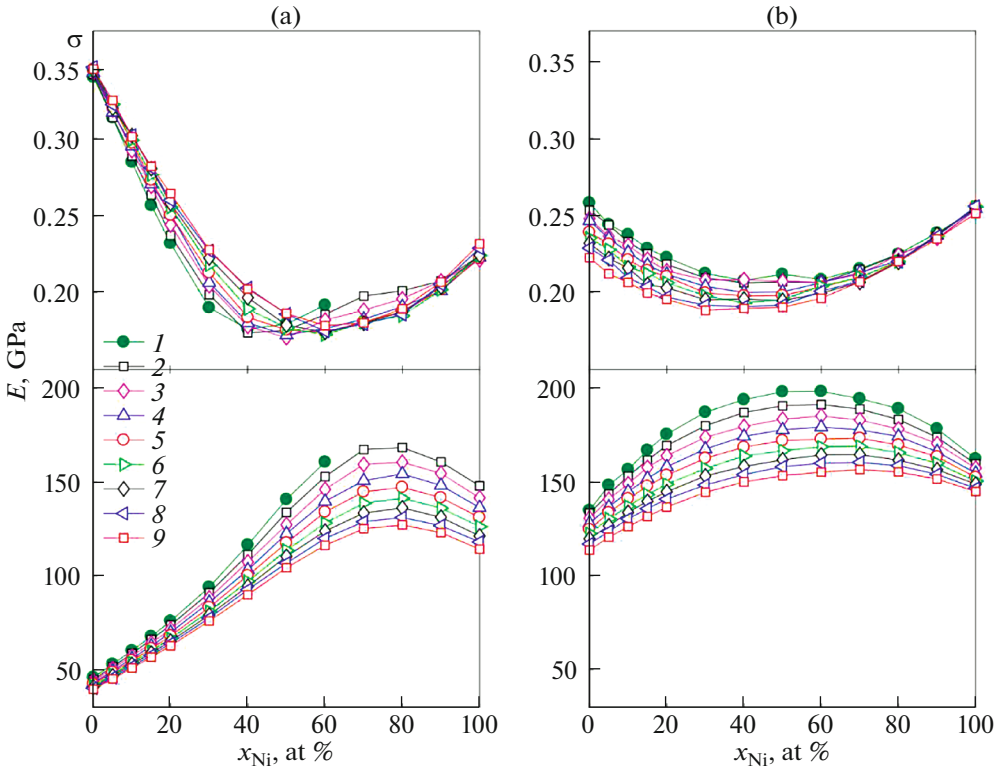

Fig. 4. Concentration dependences of Poisson's ratio and Young's modulus of aluminum-nickel (a) and iron-nickel (b) melts at different temperatures: (*1*–*9*) see Fig. 1.

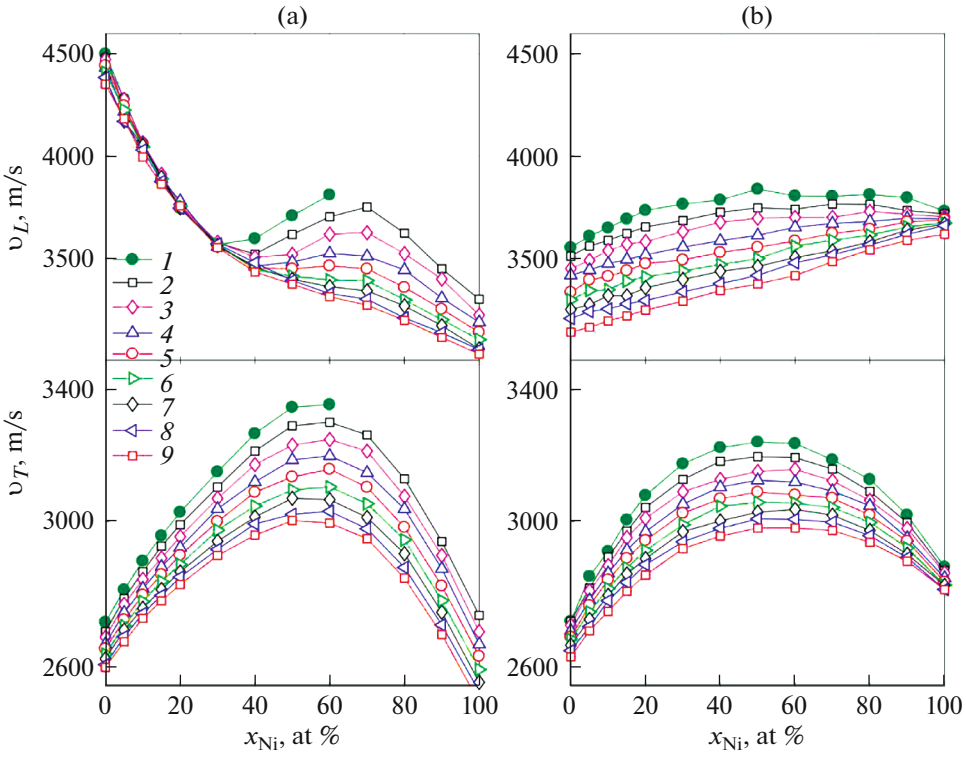

Fig. 5. Concentration dependences of the longitudinal and transverse sound velocities of $Al_{(100-x)}Ni_x$ (a) and $Fe_{(100-x)}Ni_x$ (b) melts at different temperatures: (*1*–*9*) see Fig. 1.

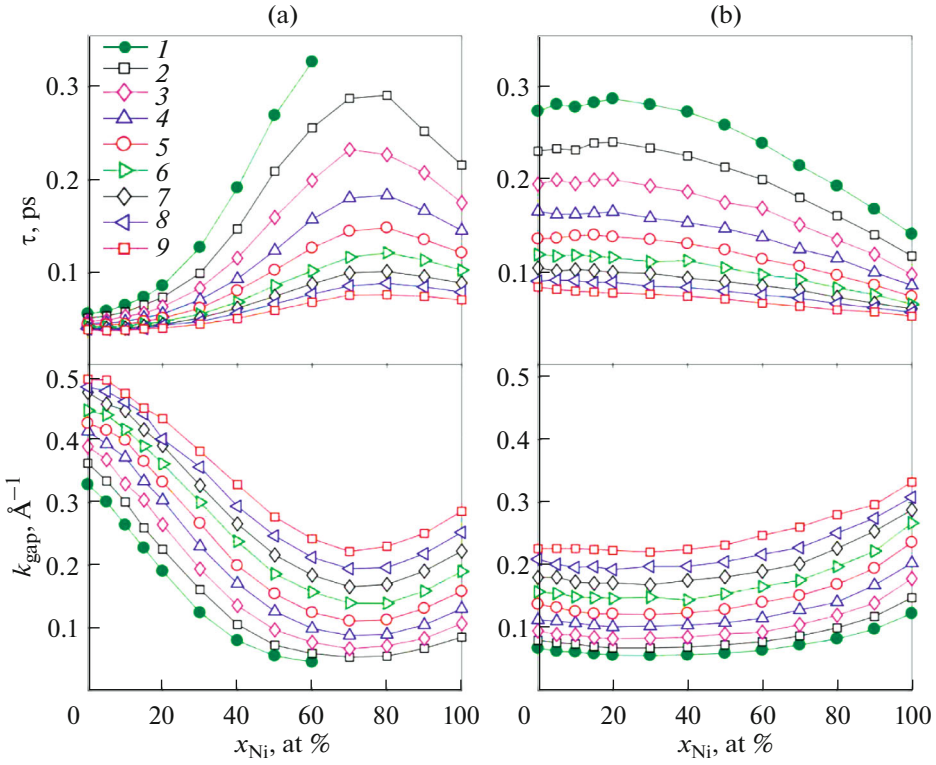

Fig. 6. Concentration dependences of the relaxation time of the viscous process and the gap width in the law of dispersion of transverse collective modes for aluminum-nickel (a) and iron-nickel (b) melts at different temperatures: (*1*–*9*) see Fig. 1.

more pronounced solid-like properties compared to $Al_{(100-x)}Ni_x$ melts.

CONCLUSIONS

The experimental measurements of viscosity and large-scale molecular dynamics studies of the viscoelastic properties and quasi-solid-state features of nickel-containing binary metal $Al_{(100-x)}Ni_x$ and $Fe_{(100-x)}Ni_x$ melts have been carried out for a wide range of temperatures, including the range of the equilibrium liquid phase and supercooled melt. A significant increase in viscosity was recorded at nickel concentrations of $x_{Ni} = 60–80\%$ and 30–50% for aluminum–nickel and iron–nickel melts, respectively. At $x_{Ni} \sim 5\%$, pronounced features were observed in the shear and kinematic viscosity of $Fe_{(100-x)}Ni_x$. The elastic properties were analyzed based on the numerical calculations of the compressive and shear moduli, Poisson's ratio, and Young's modulus. The compositions of aluminum-nickel and iron-nickel melts, for which the maximum strength properties are manifested, have been determined. The calculated concentration dependences of the velocities of longitudinal and transverse sound waves demonstrate a correlation with viscosity. It has been established that at $x_{Ni} \le 60\%$ $Fe_{(100-x)}Ni_x$ melts are characterized by more pronounced solid-like properties compared to $Al_{(100-x)}Ni_x$ melts.

ACKNOWLEDGMENTS

Large-scale molecular dynamics calculations were performed on the computational cluster of the Kazan Federal University and the supercomputer of the Interdepartmental Supercomputer Center of the Russian Academy of Sciences.

FUNDING

This study was supported by the Russian Science Foundation, project no. 19-12-00022.

CONFLICT OF INTEREST

The authors declare that they have no conflicts of interest.

REFERENCES

1. Schweitzer, P.E., *Metallic Materials: Physical, Mechanical, and Corrosion Properties*, Boca Raton: CRC, 2004.
2. Faulkner, J.S. and Jordan, R.G., *Metallic Alloys: Experimental and Theoretical Perspectives*, Dordrecht: Springer, 1994.
3. Li, F.C., Liu, T., Zhang, J.Y., Shuang, S., Wang, Q., Wang, A.D., Wang, J.G., and Yang, Y., *Mater. Today Adv.*, 2019, vol. 4, p. 100027.
4. Ovchinnikov, A., Smetana, V., and Mudring, A.-V., *J. Phys.: Condens. Matter*, 2020, vol. 32, 243002.
5. Viswanath, D.S., Ghosh, T.K., Prasad, D.H., Dutt, N.V., and Rani, K.Y., *Viscosity of Liquids: Theory, Estimation, Experiment, and Data*, Dordrecht: Springer, 2007.
6. Trachenko, K. and Brazhkin, V.V., *Sci. Adv.*, 2020, vol. 6, no. 17, p. 3747.
7. Khusnutdinov, R.M. and Mokshin, A.V., *JETP Lett.*, 2019, vol. 110, no. 8, p. 557.
8. Bellissard, J. and Egami, T., *Phys. Rev. E*, 2018, vol. 98, p. 063005.
9. Cheng, J., Grobner, J., Hort, N., Kainer, K.U., and Schmid-Fetzer, R., *Meas. Sci. Technol.*, 2014, vol. 25, p. 062001.
10. Mishin, Y., *Acta Mater.*, 2004, vol. 52, no. 6, p. 1451.
11. Bonny, G., Pasianot, R.C., and Malerba, L., *Modell. Simul. Mater. Sci. Eng.*, 2009, vol. 17, p. 025010.
12. Khusnutdinoff, R.M. and Mokshin, A.V., *J. Non-Cryst. Solids*, 2011, vol. 357, no. 7, p. 1677.
13. Bel'tyukov, A.L. and Lad'yanov, V.I., *Instrum. Exp. Tech.*, 2008, vol. 51, no. 2, p. 155.
14. Shvidkovskii, E.G., *Nekotorye voprosy vyazkosti rasplavlennykh metallov* (Some Issues of the Viscosity of Molten Metals), Moscow: Gostekhizdat, 1955.
15. Beltyukov, A., Olyanina, N., and Ladyanov, V., *J. Mol. Liq.*, 2009, vol. 281, p. 204.
16. Khusnutdinov, R.M., Mokshin, A.V., Men'shikova, S.G., Bel'tyukov, A.L., and Lad'yanov, V.I., *J. Exp. Theor. Phys.*, 2016, vol. 122, p. 859.
17. Khusnutdinoff, R.M., Mokshin, A.V., Beltyukov, A.L., and Olyanina, N.V., *Phys. Chem. Liq.*, 2018, vol. 56, p. 561.
18. Khusnutdinov, R.M., Mokshin, A.V., Bel'tyukov, A.L., and Olyanina, N.V., *High Temp.*, 2018, vol. 56, no. 2, p. 201.
19. Maret, M., Pomme, T., and Pasturel, A., *Phys. Rev. B*, 1990, vol. 42, p. 1598.
20. Das, S.K., Horbach, J., Koza, M.M., Mavilla, Chatoth S., and Meyer, A., *Appl. Phys. Lett.*, 2005, vol. 86, p. 011918.
21. Brillo, J., Bytchkov, A., Egry, I., Hennet, L., Mathiak, G., Pozdnyakova, I., Price, D.L., Thiaudiere, D., and Zanghi, D., *J. Non-Cryst. Solids*, 2006, vol. 352, p. 4008.
22. Mokshin, A.V., Khusnutdinoff, R.M., Galimzyanov, B.N., and Brazhkin, V.V., *Phys. Chem. Chem. Phys.*, 2020, vol. 22, p. 4122.
23. Kehr, M., Schick, M., Hoyer, W., and Egry, I., *High Temp.—High Pressure*, 2008, vol. 37, p. 361.
24. Levin, E.S., Petrushevskii, M.S., Gel'd, P.V., and Ayushina, G.D., *Zh. Fiz. Khim.*, 1972, vol. 45, p. 3035.
25. Sato, Y., Sugisawa, K., Aoki, D., and Yamamura, T., *Meas. Sci. Technol.*, 2005, vol. 16, p. 363.
26. Krieger, V.W. and Trenkler, H., *Arch. Eisenhuettenwes.*, 1971, vol. 42, p. 175.
27. Baum, B.A., *Metallicheskie zhidkosti* (Metallic Liquids), Moscow: Nauka, 1979.
28. Plevachuk, Y., Egry, I., Brillo, J., Holland-Moritz, D., and Kaban, I., *Int. J. Mater. Res.*, 2007, vol. 98, no. 2, p. 107.
29. Ayushina, G.D., Levin, E.S., and Gel'd, P.V., *Zh. Fiz. Khim.*, 1969, vol. 43, no. 11, p. 2756.
30. Kobatake, H. and Brillo, J., *J. Mater. Sci.*, 2013, vol. 48, p. 4934.
31. Lyapin, A.G., Gromnitskaya, E.L., Yagafarov, O.F., Stal'gorova, O.V., and Brazhkin, V.V., *J. Exp. Theor. Phys.*, 2008, vol. 107, no. 5, p. 818.
32. Trachenko, K. and Brazhkin, V.V., *Rep. Prog. Phys.*, 2016, vol. 79, p. 016502.
33. Trachenko, K., *Phys. Rev. E*, 2017, vol. 96, p. 062134.
34. Khusnutdinoff, R.M., Cockrell, C., Dicks, O.A., Jensen, A.C.S., Le, M.D., Wang, L., Dove, M.T., Mokshin, A.V., Brazhkin, V.V., and Trachenko, K., *Phys. Rev. B*, 2020, vol. 101, p. 214312.